crystals

MDPI

Article

Ivabradine Hydrochloride (*S*)-Mandelic Acid Co-Crystal: In Situ Preparation during Formulation

Veronika Sládková [1,*], Ondřej Dammer [2], Gregor Sedmak [2], Eliška Skořepová [1] and Bohumil Kratochvíl [1]

[1] Department of Solid State Chemistry, University of Chemistry and Technology Prague, Technicka 5, 16628 Prague 6, Czech Republic; skorepoe@vscht.cz (E.S.); Bohumil.Kratochvil@vscht.cz (B.K.)

[2] Zentiva, k.s., U kabelovny 130, 10237 Prague 10, Czech Republic; Ondrej.Dammer@zentiva.cz (O.D.); Gregor.Sedmak@zentiva.cz (G.S.)

* Correspondence: sladkovv@vscht.cz

Academic Editor: Srinivasulu Aitipamula

Received: 11 November 2016; Accepted: 21 December 2016; Published: 6 January 2017

Abstract: The pharmaceutical salt ivabradine hydrochloride is indicated for the symptomatic treatment of chronic stable angina pectoris and chronic heart failure. It exhibits extensive polymorphism and co-crystallization, which could be a way to provide an alternative solid form. We conducted a co-crystal screen, from which two hits were identified: with (*S*)-mandelic and (*R*)-mandelic acid. Both structures were determined from single-crystal X-ray diffraction data as co-crystals. The co-crystals were further characterized by common solid-state techniques, such as X-ray powder diffraction (XRPD), differential scanning calorimetry (DSC), solid-state NMR, IR and Raman spectroscopy, and dynamic vapor sorption (DVS). The co-crystal with (*S*)-mandelic acid was selected for further development; its physical and chemical stability was compared with two different polymorphs of the hydrochloride salt. The co-crystal exhibited a similar stability with the polymorph used in the original drug product and was, therefore, selected for formulation into the drug product. During the pre-formulation experiments, the in situ formation of the co-crystal was achieved during the wet granulation process. The following formulation experiments showed no influence of in situ prepared co-crystal on the overall stability of the bulk, when compared with pre-prepared co-crystal formulation.

Keywords: co-crystals; crystal polymorphism; crystal structure; preformulation; X-ray powder diffractometry

1. Introduction

Multicomponent solid forms of pharmaceutical substances (APIs) are widely screened from early drug development, as they provide a whole range of forms with different physicochemical properties. In addition to polymorphs, some solvates, salts, or co-crystals can be selected as desirable solid forms of API, present in the drug product. Co-crystals have captured the attention of solid-state scientists for their immense possibilities: (i) the number of co-crystal formers (co-formers) exceeds the number of counterions [1]; when multicomponent solid forms are screened for, therefore, more options are available; (ii) there is no need to force the screened pharmaceutical substance to donate or accept a proton in order to prepare a new multicomponent solid form; and (iii) combinations, such as co-crystal hydrate, co-crystal of a salt, etc., can extend the solid-state portfolio, as well.

Pharmaceutical cocrystals have been successfully studied by numerous groups, which have reported many effective co-crystal preparation techniques, such as neat grinding [2,3], liquid-assisted grinding [4] or co-melting [5,6] of co-crystal components or co-crystallization from solutions [7]. Co-crystals, solvates and salts are multicomponent solid forms and, sometimes, the boundary between

co-crystal/salt and co-crystal/solvate is indistinct. Determination of crystal structure enables to understand and distinguish between these forms. Also ionic compounds (i.e., salts), can form molecular complexes with neutral molecules, forming a co-crystal of a salt (also known as ionic co-crystal) [8,9] or a solvated/hydrated salt [10,11]. An example of a salt forming co-crystals is fluoxetine hydrochloride, forming several co-crystals with carboxylic acids [12]. Not only API hydrochlorides can form co-crystals, but also co-crystals of chlorides of API have been reported, such as co-crystals of trospium chloride [13,14]. The formation of mixed salt-co-crystals, in which the API forms a co-crystal with its own salt, has been also reported [15]. In such systems, the API can act as either an acid (e.g., valproic acid sodium valproate salt-co-crystal [15]) or a base (e.g., tiotropium fumarate fumaric acid salt-co-crystal [16]). While it has not been proven that co-crystals are a solution to polymorphism (as co-crystals also exhibit polymorphism) [17,18], they certainly can offer an alternative solid form, especially in generic pharmaceutical development.

Ivabradine hydrochloride (Figure 1, IVA HCl) [19] is used for the treatment of chronic stable angina pectoris and a chronic heart failure and is marketed under trade name Procorolan in doses of 5 and 7.5 mg by Servier Laboratories. IVA HCl is present as the polymorphic form γ in the original drug product [20]. However, Servier also patented other polymorphic forms which were denoted as forms α, β, βd, γd, δ, and δd [21–25]. Other pharmaceutical companies (Krka, Cadila) patented several polymorphs with different designations: forms ε and ζ [26,27], form I–form IV, forms Z, X and K, form C and S [28–33]. Moreover, acetone and acetonitrile solvates [34] and different salts of ivabradine, such as hydrobromide, oxalate, sulfate, adipate, and tartrate [35–39] are described in the patent literature.

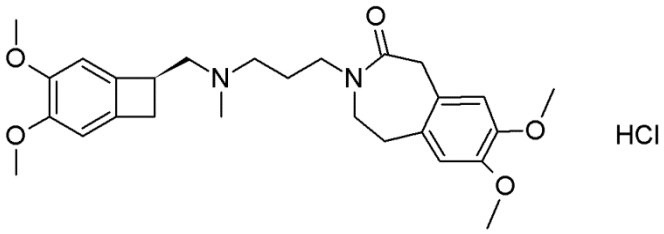

Figure 1. Molecular formula of ivabradine hydrochloride.

This paper describes the development of a generic product containing a co-crystal. At the beginning of the project, several patent-free polymorphic forms of IVA HCl were available on the market from different suppliers. However, internal analysis (by Zentiva) showed that many of the marketed forms were identical with forms described and patented by originators (Servier Laboratories, e.g., form δd) or they corresponded to the mixtures containing the originator's polymorphic form(s). Only polymorphic form II showed to be polymorphically pure and was used for further pharmaceutical development. However, conversion of form II into form γ present in the original drug product Procorolan was observed during the stability treatment (this part is not included in the paper). Therefore, we decided to screen IVA HCl for co-crystals, characterize the obtained hits by several solid state techniques (X-ray powder diffraction (XRPD), single-crystal X-ray diffraction (SXRD), solid-state nuclear magnetic resonance (ssNMR), differential scanning calorimetry (DSC), and dynamic vapor sorption (DVS)), select one co-crystal for further pharmaceutical development and suggest physically and chemically stable pharmaceutical compositions containing the co-crystal. Furthermore, ethanol solvate of ivabradine hydrochloride was also prepared, characterized and its crystal structure was determined. Moreover, the physicochemical properties of the co-crystal selected for pharmaceutical development (with (*S*)-mandelic acid) were compared with the polymorphic form γ present in the original drug product and form II used at early stages of our pharmaceutical development.

We also show that the co-crystal can be manufactured in situ during the formulation process. Simple wet granulation of IVA HCl, co-former, and excipients led to the formation of the co-crystal

without the detection of any input components. Such an approach seems to be very promising for robust co-crystal manufacturing compared to the described technology-spray drying [40] or twin screw extrusion [41].

It should also be noted that the structures of ivabradine hydrochloride forms remain elusive, and only the structure of polymorph β is deposited in the Cambridge Structure Database (CSD) [42] under reference RIYKIT and is determined as tetrahydrate [43]. The structure of form II was also solved and published directly in the patent, however, the structure is not available in CSD [44]. Form γ seems to be a monohydrate [20]; form δ is a non-stoichiometric hydrate comprising about 2.8% of water [25]. The other forms are anhydrous, but the structures are yet to be determined. The successful indexing of forms α, βd, and δd was done by Masciocchi et al.; in their publication they also revealed indexed powders of acetone and acetonitrile solvates δd_1 and δd_2 [45].

2. Experimental Section

2.1. Materials

Ivabradine hydrochloride (IVA HCl) in form δd and form II, and the excipients, were kindly provided by Zentiva k.s. (Prague, Czech Republic).

Solvents and co-crystal formers were purchased from various suppliers and were used as received. Most of co-formers were purchased from Sigma Aldrich (St. Louis, MO, USA); benzoic, fumaric and oxalic acid from Alfa Aesar (Ward Hill, MA, USA); camphoric and salicylic acids from Fluka (St. Louis, MO, USA), and benzenesulfonic, pamoic acids from Acros organics (Geel, Belgium). All co-formers have purity higher than 99%.

2.2. Analytical Methods

2.2.1. Powder X-ray Diffraction (XRPD)

Fast X-ray powder diffraction data for screening experiments were collected at room temperature with a laboratory X'PERT PRO MPD PANalytical diffractometer (PANalytical, Almelo, The Netherlands) with parafocusing Bragg-Brentano geometry, using CuKα radiation (λ = 1.54184 Å), with a measurement range of 2−40° 2θ, a step size of 0.01° 2θ, and a counting time of 0.5 s·step^{-1}. Samples were ground in an agate mortar and stacked on a Si holder (zero background). Data evaluation was performed in the software package HighScore Plus.

2.2.2. Infrared (IR) Spectroscopy

ATR (ZnSe—single reflection) infrared spectra of the solids were obtained using an infrared spectrometer equipped with a deuterated-triglycine sulfate (DTGS) detector and KBr beam splitter. A total of 12 scans per spectrum were acquired in the range 4000–600 cm^{-1}. Spectral resolution was 2 cm^{-1}. The data were acquired and interpreted using Omnic 6.2.

2.2.3. Raman Spectroscopy

Raman spectroscopic analyses were carried out on a FT-Raman RFS100/S spectrometer equipped with a germanium detector (Bruker Optics, Ettlingen, Germany). Spectra were collected using an excitation wavelength of 1064 nm of Nd:YAG laser radiation (power 250 mW). Each sample was analyzed in a High Performance Liquid Chromatography (HPLC) glass vial. A total of 64 scans per spectrum were acquired from 4000 to −2000 cm^{-1}. Spectral resolution was 4 cm^{-1}. The data were acquired and interpreted using Opus 5.5.

2.2.4. Solution Nuclear Magnetic Resonance (Solution NMR)

Solution NMR was used for identification of the compounds and to determine the chemical purity, impurities, and stoichiometry of the prepared materials. Samples were dissolved in dry d6-DMSO

and ^{1}H NMR spectra were measured by a Bruker Avance III™ 500 MHz NMR spectrometer ((Bruker BioSpin, Rheinstetten, Germany) equipped with a Prodigy probe and with a repetition delay of 10 s.

2.2.5. Solid-State Nuclear Magnetic Resonance (ssNMR)

Solid-state 13C NMR was used to provide the phase identification, phase purity of the prepared materials, and to study the solid state transformations. ^{13}C NMR spectra were measured by a Bruker Avance III™ 400 MHz WB by CPMAS (298 K, spinning rate of 13 kHz, relaxation delay of 5 s) equipped with a 4 mm probe. The necessary number of scans was approximately 1000. Glycine was used as the external standard.

2.2.6. Differential Scanning Calorimetry (DSC)

DSC measurements were performed on a PerkinElmer Pyris 1 DSC (PerkinElmer, Waltham, MA, USA). The sample were weighed in aluminum pans and covered and measured in a nitrogen flow (20 mL/min). Investigations were performed in a temperature range of 50−200 °C with a heating rate of 10 °C/min. The temperatures specified in relation to DSC analyses are the onset temperatures of peaks. The specific heat is given in J/g. The weight of the sample was approximately 3 mg.

2.2.7. Dynamic Vapor Sorption (DVS)

Dynamic vapor sorption (DVS) was measured on a DVS Advantage 1 device (Surface Measurement Systems, London, UK) from Surface Measurement Systems. The sample weight in a quartz crucible was between 20.3 and 21.1 mg, and the temperature in the device was kept between 25.3 and 25.4 °C. The used measuring program is as follows: the sample was measured by one cycle, from 0% relative humidity (RH) to 90% relative humidity (adsorption) and then from 90% relative humidity to 0% relative humidity (desorption). As measuring gas 4.0 nitrogen flow of 200 sccm was used. Step in RH change was 10%, and the sample was kept at each level of RH until its weight ceased deviating. When the sample weight did not change, the humidity was increased/decreased during sorption/desorption.

2.2.8. Karl Fischer Coulometric Titration

The water mass fraction was determined using a Karl Fischer coulometer (652 model, Metrohm AG, Bleiche West, Switzerland) equipped with an E649 magnetic stirrer. The measurements were done in accordance with European Pharmacopoeia [46] and each was repeated three times to obtain an average value.

2.2.9. Single Crystal X-ray Diffraction (SXRD)

The single crystals of co-crystals ivabradine hydrochloride (*S*)-mandelic acid (IClSM), and ivabradine hydrochloride (*R*)-mandelic acid (IClRM) for structure determination were obtained by spontaneous cooling of hot co-crystal solutions (from 70 °C to RT) in ethanol. The preparation of ivabradine hydrochloride ethanol solvate (IClEt) was serendipitous and the single crystals were obtained from a suspension of ivabradine hydrochloride in ethanol. When the measured XRPD pattern did not match with other previously described forms, the single crystals were measured by SXRD. The phase was not reproduced.

The analysis was conducted using the Xcalibur, Atlas, Gemini ultra diffractometer with a mirror monochromator and a CCD detector, with Cu Kα radiation with the wavelength of 1.5418 Å. The data were collected and reduced by the CrysAlisPro program by Agilent Technologies, version 1.171.36.28. The SCALE3 ABSPAC scaling algorithm was used for empirical correction to absorption.

The structure was solved by a direct method SIR92 and refined in CRYSTALS 14.40b. All non-hydrogen atoms were refined with anisotropic thermal displacement parameters.

2.2.10. Ultra Performance Liquid Chromatography (UPLC)

The chemical purity was determined by liquid chromatography. The samples were analyzed by UPLC (Acquity) equipped with an Acquity UPLC BEH C18 column (1.7 μm, 2.1 mm × 100 mm), at a column temperature of 45 °C. As the mobile phase a mixture of 10 mM ammonium carbonate buffer, pH 10.2, and methanol was used, (gradient program: time/min: 0-15-17-21-21.5-24 methanol/%: 10-60-80-80-10-10) at a flow rate of 0.35 mL/min. In the analysis, 2.0 mL of a liquid sample containing 50% methanol as solvent was dispensed in the column (stock solution concentration 0.75 mg/mL). For UV detection absorption at 288 nm was used.

2.3. Sample Preparation

2.3.1. Co-Crystal Screening

The co-crystal screening of ivabradine hydrochloride (IVA HCl) was conducted with 28 coformers: adipic acid, aminosalicylic acid, ascorbic acid, benzenesulfonic acid, benzoic acid, camphoric acid, cinnamic acid, citric acid, fumaric acid, gentisic acid, glutaric acid, hippuric acid, isonicotinamide, lysine, maleic acid, malic acid, malonic acid, (*S*)-mandelic acid, (*R*)-mandelic acid, nicotinamide, nicotinic acid, oxalic acid (dihydrate), pamoic acid, saccharin, salicylic acid, succinic acid, tartaric acid, and vanillin. Equimolar mixtures of API (20 mg) and a co-former were placed in 50-mL round-bottomed flasks, dissolved in ethanol at ambient temperature, and left until crystalline material was formed. The resulting solids were then analyzed by X-ray powder diffraction (XRPD).

2.3.2. Co-Crystal Reproduction

Hits obtained during the screen were reproduced by two co-crystallization techniques: by slurrying (100 mg of API and co-former in equimolar ratio) in 2 mL of acetone, dioxane, DMSO, ethanol, ethyl acetate, and methanol (slurried for 48 h), and liquid-assisted grinding (LAG, same amount as for slurrying) with 0.2 mL of ethanol, ethyl acetate, and acetone (ground in a mortar and pestle for 10 min).

2.3.3. Maturation Experiments

As co-crystal was formed with enantiomerically pure (*S*)-mandelic (IClSM) or (*R*)-mandelic acid (IClRM), and we wondered what would be the resulting solid of co-crystallization of ivabradine hydrochloride with racemic mandelic acid. In such a case, three outcomes would be possible: IClSM, IClRM, or a novel form incorporating the racemic mandelic acid. Mixtures of IVA HCl with an excess of racemic mandelic acid (100 mg of the mixture in 1:2 molar ratio) were slurried for two weeks (in 1 mL of ethanol and ethyl acetate) and the resulting solids were identified using XRPD.

2.3.4. Long-Term Physical Stability Studies of IClSM

The stability of IClSM co-crystal and IVA HCl δd was tested at two different conditions: 25 °C/60% RH and 40 °C/75% RH. The solid was sampled after two weeks, one month, and three months, and analyzed by XRPD.

2.3.5. Physical and Chemical Stability: Stress Studies

The powders of co-crystal IClSM, ivabradine hydrochloride form II, and form γ were stressed for three days at 80 °C and 0% RH, three days at 80 °C and 75% RH, 10 days at 0% RH, and 10 days at 100% RH. Chemical stability (content of impurities) was evaluated by UPLC, and physical stability (polymorphic purity) was evaluated by XRPD. For quantification of the phase admixtures the standard addition method was applied.

2.3.6. Pre-Formulation of Ivabradine Hydrochloride (*S*)-Mandelic Acid Co-Crystal (IClSM)

Stoichiometric amounts of IVA HCl and (*S*)-mandelic acid with excess of lactose monohydrate was mixed in a beaker or vial with spatula. Using a micropipette, ethanol (EtOH) or water (WA) was added as the granulation liquid. We wanted to achieve conditions for wet granulation at a small laboratory scale. Table 1 shows the amount of used components.

Table 1. The composition of the wet-granulated pre-formulation mixtures.

Experiment	IVA HCl (mg)	(*S*)-Mandelic Acid (mg)	Lactose Monohydrate (mg)	Solvent	
				Type	Amount (µL)
Liquid-assisted grinding (LAG)	100	30	-	EtOH	50
	100	30	-	WA	40
	200	60	-	WA	20
Mixing in a vial by microspatula	10	3	130	EtOH	30
	10	3	130	EtOH	60
	10	3	130	EtOH	100
	10	3	130	WA	30
	10	3	130	WA	70
	100	30	1300	EtOH	50
	100	30	1300	EtOH	100
	100	30	1300	EtOH	150
	100	30	1300	EtOH	200
High-shear granulation *	300	90	4000	EtOH	1200
	300	90	4000	EtOH	1800
	300	90	4000	EtOH	2100
Mixing in a beaker	750	225	10,000	EtOH	560

* High-shear granulation was simulated in a stainless steel cell (see Figure S16 in Supplementary Material), in which a thick mixture of co-crystal components and filler (lactose monohydrate) was intensively kneaded by an overhead stirrer (960 rpm).

2.4. Formulation

The co-crystal IClSM formulated with excipients was either pre-prepared (mixtures A–C), or it was formed directly during the wet granulation in the presence of the excipients (mixtures D–J). For mixtures A–C, all of the components were mixed in a beaker using a spatula for 15 min. Then, we added ethanol (37 mg of ethanol per tablet weight) and continued mixing for an additional 15 min. For mixtures D–F, all of the components, except magnesium (Mg) stearate, were granulated by ethanol in a beaker, using a spatula, at the same time. The granulates were dried in air for 2 h. Then, to the dried granules, Mg stearate was added. For mixtures G–H, all of the components, except meglumine and Mg stearate, were granulated by ethanol and let to dry. Then, to the dried granules, first meglumine, then Mg stearate, were gradually added. For mixtures I–J, BHT/citric acid were dissolved in ethanol, by which all the components, except Mg stearate, were granulated and dried. Then, to the dried granules, Mg stearate was added. The compositions of the mixtures A–J are shown in Tables 2 and 3.

Table 2. The composition of the mixtures A–C with pre-prepared co-crystal.

Ingredient (mg)	A	B	C
IClSM	10.5	10.5	10.5
Klucel EF	2.7	2.7	2.7
Lactose monohydrate	115.0	-	111.9
Mannitol	-	115	-
Primojel type A	5.4	5.4	5.4
Meglumine	-	-	3.125
Magnesium stearate	1.35	1.35	1.35
Tablet weight (mg)	135	135	135

Table 3. The composition of the mixtures D–J with co-crystal formed in situ.

Ingredient (mg)	D	E	F	G	H	I	J
Ivabradine HCl	8.085	8.085	8.085	8.085	8.085	8.085	8.085
(*S*)-mandelic acid	2.436	2.436	2.436	2.436	2.436	2.436	2.436
Klucel EF	2.7	2.7	2.7	2.7	2.7	2.7	2.7
Lactose monohydrate	115.0	-	112.3	114.25	111.9	114.8	111.5
Mannitol	-	115	-	-	-	-	-
Primojel type A	5.4	5.4	5.4	5.4	5.4	5.4	5.4
Butylhydroxytoluene(BHT)	-	-	-	-	-	0.27	-
Citric acid	-	-	-	-	-	-	3.5
Meglumine	-	-	-	0.781	3.125	-	-
Magnesium stearate	1.35	1.35	4.05	1.35	1.35	1.35	1.35
Tablet weight (mg)	135	135	135	135	135	135	135

Characterization of Mixtures A–J

Initial characterization: The prepared mixtures were firstly characterized by pH measurement, water content determination and chemical (UPLC), and physical (XRPD) purity. All mixtures were dried at 40 °C for 90 min for water content determination by Karl-Fisher titration. Approximately 2.5 g of the mixture was used for one measurement. The mean value of three measurements was used as the determined water content. For pH determination, 200 mg of the respective mixtures of A–J was placed in a vial, 10 mL of purified water was added, and pH was measured by a Microprocessor pH meter 213 (HANNA Instruments). The mixtures were packed in aluminum sachets, filled with either air or nitrogen atmosphere and stressed with a temperature of 80 °C for a duration of 72 h in a stability chamber (Memmert HCP 108). The physical and chemical purity was analyzed by XRPD and UPLC.

3. Results and Discussion

3.1. Co-Crystal Screening and Solid-State Characterization of Hits

We performed the co-crystal screening of ivabradine hydrochloride; the resulting solids were measured by XRPD and two unique powder patterns (differing from the patterns of input components) were identified. The new powder patterns were also compared with available XRPD patterns of different polymorphs of IVA HCl, so their uniqueness was confirmed. When single crystals were obtained, the structures were determined from SXRD data as ivabradine hydrochloride (*S*)-mandelic acid 1:1 co-crystal (IClSM) and ivabradine hydrochloride (*R*)-mandelic acid 1:1 co-crystal (IClRM). The co-crystals were reproduced by other co-crystallization techniques: slurrying and liquid-assisted grinding in a range of solvents. The solid-state characterization, such as differential scanning calorimetry (DSC), solid-state NMR (ssNMR), IR and Raman spectroscopy, and dynamic vapor sorption (DVS), for both co-crystals followed. The figures and comments discussing the observations from the solid state characterization (XRPD, IR and Raman spectroscopy, DSC, and DVS) are available in detail in the Supplementary Material (Figures S1–S15). Both co-crystals showed low hygroscopicity and distinct melting temperature, comparable with polymorphic form γ, which was identified in the drug product of the originator.

3.2. Crystal Structures and Their Comparison

The crystal structures of ivabradine hydrochloride (*S*)-mandelic acid 1:1 co-crystal (IClSM), ivabradine hydrochloride (*R*)-mandelic acid 1:1 co-crystal (IClRM), and of ivabradine hydrochloride ethanol solvate (IClEt) were solved from single-crystal X-ray diffraction (SXRD) data (Table 4 and Figure 2).

Table 4. Crystallographic data of IClSM, IClRM, and ivabradine hydrochloride ethanol solvate (IClEt).

Compound	IClSM	IClRM	IClEt
Empirical formula	$C_{27}H_{37}N_2O_5\cdots Cl \cdot\cdot C_8H_8O_3$	$C_{27}H_{37}N_2O_5\cdots Cl \cdot\cdot C_8H_8O_3$	$C_{27}H_{37}N_2O_5\cdots Cl \cdot\cdot C_2H_6O$
Formula wt.	657.20	657.20	551.12
Crystal system	Orthorhombic	Orthorhombic	Monoclinic
Space group	$P\,2_12_12_1$	$P\,2_12_12_1$	$P\,2_1$
a (Å)	7.4447(4)	7.5398(2)	5.4844(10)
b (Å)	8.5027(4)	8.6296(2)	11.7967(10)
c (Å)	52.159(2)	51.5013(13)	21.8297(10)
β (°)	90	90	91.905(10)
V (Å^3)	3301.67(13)	3350.96(8)	1411.55(6)
Z	4	4	2
T (K)	120	120	100
ρ_{calc} (g·cm^{-3})	1.322	1.303	1.297
Radiation	CuKα (1.5418 Å)	CuKα (1.5418 Å)	CuKα (1.5418 Å)
μ (mm^{-1})	1.477	1.456	1.565
F(000)	1400.0	1400.0	592.0
Reflns collected	12,420	11,567	20,662
Indep. Reflns (R_{int})	5425 (0.057)	5853 (0.035)	5586 (0.083)
GOF	0.962	1.039	1.160
R1, wR2 [I>2σ(I)]	0.045, 0.062	0.043, 0.056	0.049, 0.082
R1, wR2 (all data)	0.057, 0.067	0.046, 0.057	0.052, 0.084
Res. el. dens. (e·Å^{-3})	0.36, −0.32	0.44, −0.33	0.38, −0.34
CCDC number	1,479,092	1,479,091	1,479,090

The molecule of ivabradine contains, in its structure, two nitrogen atoms (in cyclic amidic and acyclic tertiary amino groups, see Figure 1). The SXRD structure solution clearly showed that, upon hydrochloride formation, the ivabradine is protonated on the acyclic amino nitrogen (see Figure 2, left part). When co-crystallized with mandelic acid, the cyclic amidic nitrogen was not protonated. Amides are generally considered as non-ionizable, even though there are some exceptions [47]. The pK_a of the protonated N atom in an amide group would be somewhere around −8 (i.e., extremely unlikely to be protonated). In fact, in amides, upon cation formation, the oxygen atom is more likely to be protonated with pK_a of around −1. The pK_a of mandelic acid is 3.41, so the ΔpK_a would equal either −11.41 for the N, or −4.41 for the O atom. Both of these results point firmly to co-crystal territory. Together with other indicators, such as C–O bond lengths in the carboxylic group and the residual electron density near this group, this confirms the co-crystalline character of IClSM and IClRM.

Therefore, in the asymmetric unit, all of the structures contained a molecule of protonated ivabradine, a chloride anion, and a molecule of a neutral coformer/solvent. The co-crystals IClSM and IClRM crystallized in the orthorhombic system (space group $P\,2_12_12_1$) and the ethanol solvate IClEt crystallized in the monoclinic system (space group $P\,2_1$).

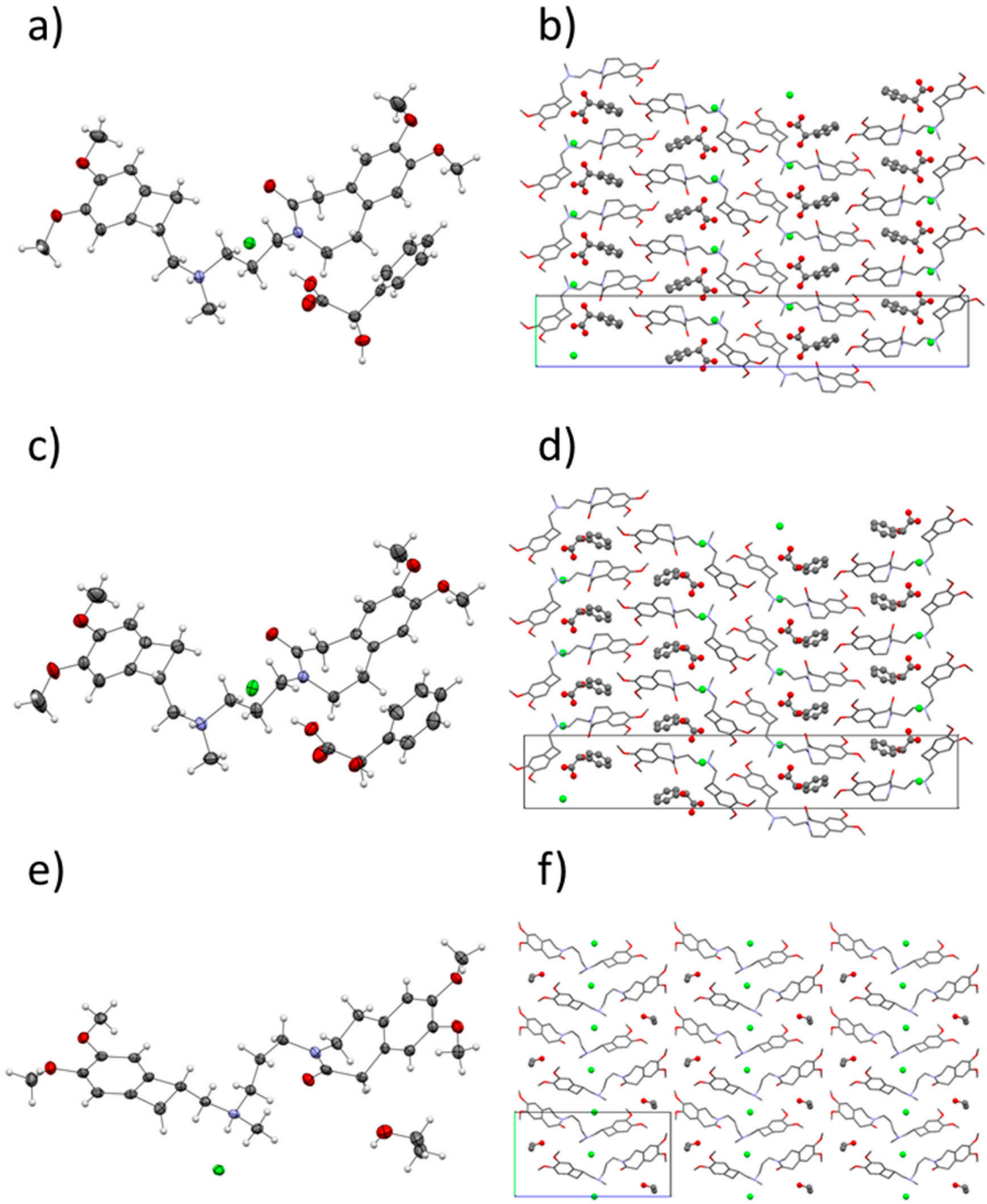

Figure 2. Crystal structures of IClSM (**a**,**b**), IClRM (**c**,**d**) and IClEt (**e**,**f**). Left: the asymmetric unit with the thermal ellipsoids. Right: the crystal packing with the unit cell.

In IClSM (Figure 3a), the (*S*)-mandelic acid forms two hydrogen bonds with the neighboring chloride anions. The protonated ivabradine nitrogen forms a weaker interaction with the chloride anion.

In IClRM (Figure 3b), the (*R*)-mandelic acid forms a hydrogen bonds to the chloride anion via its carboxyl group and to ivabradine carbonyl oxygen *via* the hydroxyl group. Ivabradine N–H is H-bond to the chloride anion.

In IClEt (Figure 3c), ivabradine N–H is also H-bonded to the chloride anion. Ethanol hydroxyl forms a weaker interaction with the ivabradine methoxy group.

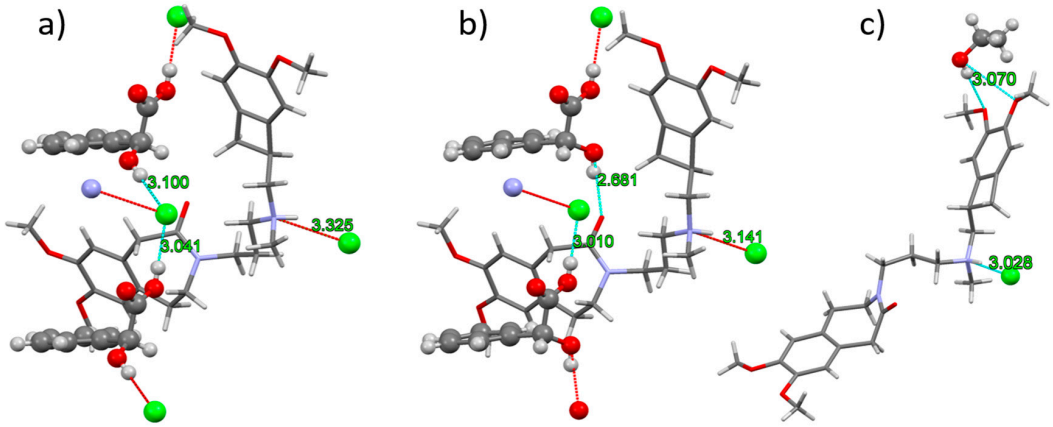

Figure 3. H-bonding in the crystal structures of IClSM (**a**), IClRM (**b**), and IClEt (**c**). The ivabradine molecule is displayed as sticks, and the rest of the structures as balls. Cyan and red dashed lines represent extended and non-extended contacts, respectively. Contact D–A distances are written in green. An extended criterion for the display of the contacts (actual D–A distance is a maximum of 3.4 Å) was used to display all of the corresponding H-bonds.

All discussed non-bonded interactions observed in SXRD correspond very well with the infrared and Raman spectroscopic data (see Supplementary Material).

Curiously, the crystal packing of IClSM and IClRM are almost identical (see Figure 2). Even though there are slight differences in the H-bonding caused by a different orientations of the hydroxyl in the (*S*)- and (*R*)-mandelic acid (see Figure 3), overall, the H-bond systems in both structures are similar as well. This could be one of the factors contributing to the high similarity in the crystal packing.

Based on the calculated crystal density, IClSM should be more thermodynamically stable than IClRM. This correlates with the experimental results because IClSM was easier to prepare than IClRM.

3.3. Co-Crystal Selection and Comparison with Other Forms of IVA HCl

From the prepared novel solid forms we had to select the most suitable one for further formulation development. As was described in the above section, the crystal structure of IClSM suggested higher density over IClRM. The reproducibility of the formation of both co-crystals was tested by two co-crystallization techniques: by slurrying and liquid-assisted grinding (LAG) in various solvents. While IClSM was reproduced by both LAG and slurrying in all solvents, co-crystal IClRM was reproduced by both methods, however, in a lower number of solvents. IClSM was always physically pure, while IClRM was often contaminated by input components ivabradine hydrochloride and (*R*)-mandelic acid. Additionally, the maturation experiment, where ivabradine hydrochloride was exposed to the excess of racemic mandelic acid, suggested that IClSM was preferred over IClRM, as it was the prevalent resulting solid form. Moreover, co-crystal IClSM exhibited a higher melting point and slightly higher density.

For all of the above-mentioned reasons, co-crystal IClSM was selected for further development and its stability was compared with other polymorphic forms of ivabradine hydrochloride, form γ and form II. During the short-term stress stability studies (when the forms were stressed for three days at 80 °C and 0% and 75% RH, and 10 days at RT at 0% RH and at 100% RH), the chemical and physical stability of pure co-crystal IClSM was compared with IVA HCl in polymorphs II and γ. Form II was chosen as a representative metastable polymorph (based on previous formulation development), while form γ was identified in the original drug product. The studies revealed that metastable form II is physically and chemically unstable. We observed the transformation of form II into polymorphic form γ (three days, 80 °C/75% RH) or into form β (10 days, 25 °C/100% RH) and the increase of chemical impurities, especially after three days at 80 °C/75% RH. On the other hand, co-crystal IClSM and form

γ were stable (see Table 5). Moreover, the conversion of form γ was observed after 10 days at 100% RH, while the co-crystal was stable. The long-term stability of the co-crystal was also initiated; see Table S1 in Supplementary Material.

Table 5. The comparison of physical and chemical stability of different solid forms of ivabradine hydrochloride (polymorphic forms II, **γ,** and co-crystal) after the treatment at various temperatures and humidities.

Stress Conditions	Form II		Form γ		Cocrystal	
	Solid Form, XRPD	Sum of Chem. Imp. [%]	Solid Form, XRPD	Sum of Chem. Imp. [%]	Solid Form, XRPD	Sum of Chem. Imp. [%]
3 days 80 °C	Form II + γ	0.15	Form γ	≤0.05	Cocrystal	≤0.05
3 days 80 °C/75% RH	Form γ	2.12	Form γ	≤0.05	Cocrystal	≤0.05
10 days 0% RH	Form II	0.15	Form γ	≤0.05	Cocrystal	≤0.05
10 days 100% RH	Form β	0.14	Form β	≤0.05	Cocrystal	≤0.05

3.4. In Situ Formation of the Co-Crystal during Wet Granulation

The preformulation experiments followed the previous knowledge about the formation of co-crystal during LAG. Therefore, we added to the mixture of API and co-former the most common formulation filler (lactose monohydrate) and tried to granulate it with two different granulation liquids (water, ethanol). We were interested if the co-crystal would also be formed in the presence of lactose monohydrate, which should simulate all excipients in a dosage form.

When granulated with water, no co-crystal formation was observed in the presence of lactose monohydrate. On the other hand, formation of co-crystal was observed when the mixture was granulated with ethanol and the co-crystal was identified by both XRPD (see Figures S17–19 in Supplementary Material) and ssNMR (see Figure 4). The initial experiments in small scale in the vial were successfully scaled-up in our own devised small scale high-shear granulator (see Figure S16 in the Supplementary Material) with, approximately, a 5 g load and even in a beaker with a load of approximately 12 g.

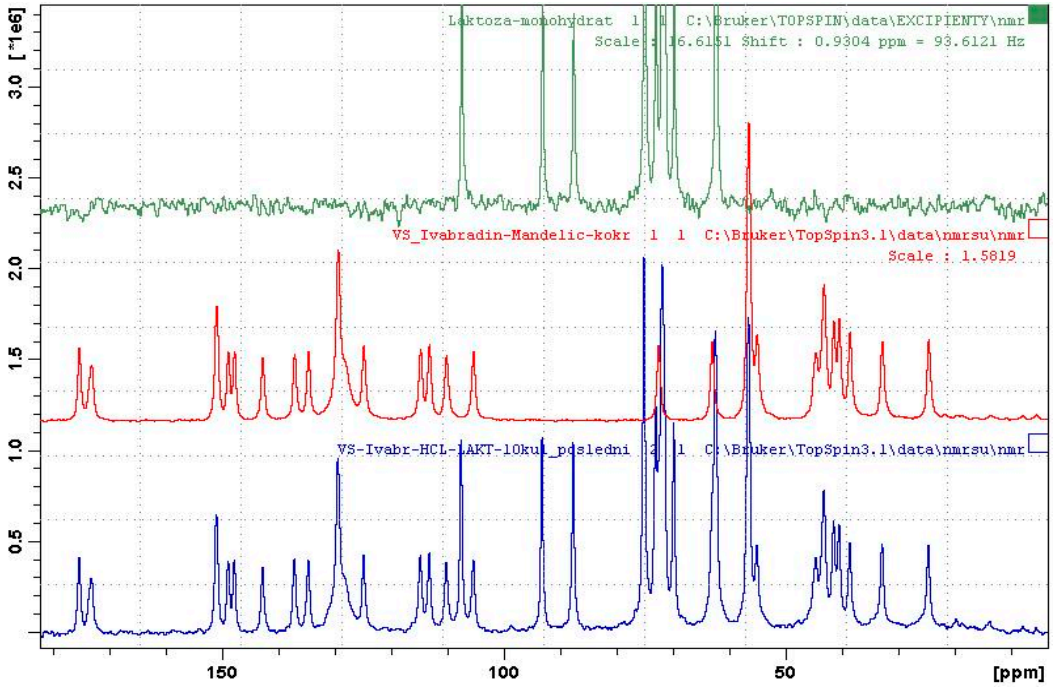

Figure 4. The ^{13}C ss NMR spectra of lactose monohydrate (**top**), co-crystal IClSM (**middle**), and EtOH-granulated mixture (**bottom**).

Figure 4 shows the ssNMR spectra of a mixture containing co-crystal, which was obtained by granulation with ethanol and the spectra of pure co-crystal and lactose monohydrate for comparison. It is evident that the spectrum of the mixture is a superposition of the spectra of lactose and the co-crystal. The ssNMR method showed to be more sensitive than traditionally-used XRPD, since lactose monohydrate exhibits long relaxation time [48] and, hence, gives a low-intensity spectrum, which does not overlap with co-crystal signals. It is the main problem of XRPD, where intense diffraction peaks of lactose monohydrate overlap the peaks of the co-crystal. Thus, ssNMR provided clear evidence of the complete conversion of hydrochloride salt into the co-crystal.

A robust reproducible in situ preparation of co-crystal IClSM in the presence of excipient(s) simplified the development of a generic product since no drug master file was necessary. We showed that suitable formulation technology (wet granulation) led to the formation of the required solid form (co-crystal).

3.5. Comparison of Pre-Prepared and in Situ Formed Co-Crystal in Formulation and Selection of Final Excipients Composition

Formulation mixtures consisting of in situ prepared co-crystal with excipients were also proposed (mixtures D–J, see Tables 2 and 3). Moreover, we investigated the physical and chemical stability of IClSM co-crystal in these in situ formed co-crystal formulations and compared it with formulations containing pre-prepared co-crystal (mixture A–C). Several formulations containing pre-prepared and in situ-formed co-crystal were suggested: the mixtures A, B, and C with pre-prepared co-crystal had identical compositions as mixtures D, E, and H, respectively, where co-crystal was prepared in situ (see Table 1 in the Experimental Section). In mixtures A and D, the filler lactose monohydrate was used; in mixtures B and E the filler mannitol was used instead of lactose. In mixtures C and H meglumine was added for the pH adjustment. In addition to these, mixture F with higher amount of Mg stearate, mixture G with a low content of meglumine, mixture I with butylhydroxytoluene as an antioxidant and mixture J with citric acid as antioxidant, were also proposed.

The mixtures were packed into aluminum blister under ambient and nitrogen atmosphere and treated for 72 h at 80 °C. The stressed mixtures were analyzed by XRPD and UPLC to predict the physical and chemical stability of the co-crystal.

The treated mixtures with pre-prepared co-crystal showed physical (mixtures A, B) or chemical instability (mixture C). In case of physical instability, we observed dissociation of the co-crystal into the γ polymorph of ivabradine hydrochloride. In the case of chemical instability, we detected chemical impurities formed by oxidative reactions. Two of them, with retention time 0.92 and 0.97, were identified by mass spectroscopy.

The treated mixtures containing in situ formed co-crystal and meglumine (mixtures G and H) were both chemically and physically unstable. Mixtures D and F were physically unstable (formation of γ form), whereas mixture J was chemically unstable. However, two suggested mixtures, namely E and I, were complying—no physical conversion and no formation of chemical impurities were observed. A detailed comparison of mixtures E and I revealed that the presence of antioxidant (butylhydroxytoluene) helped with chemical stabilization, since no increase of chemical impurities was observed after three days at 80 °C.

From the overall comparison of the mixtures with pre-prepared co-crystal with the mixtures with in situ formed co-crystal, we deduced that in situ formation of the co-crystal during the wet granulation process can be used for manufacturing. We selected a final composition for further formulation development containing co-crystal, lactose monohydrate, klucel, primojel, magnesium stearate, and butylhydroxytoluene.

Furthermore, we investigated a possible impact of water content and pH of the mixtures on the described stability. The water content was determined by Karl-Fisher titration and the results are summarized in Table S2 in Supplementary Material. The water content is between 4.3% and 4.5% for mixtures containing lactose monohydrate (crystal water) and 0.1%–0.3% for mixtures with mannitol

(mixtures B and E). Mixtures with meglumine (mixtures G and H) and with mannitol (mixtures C and F) showed higher pH than mixtures A, B, D, E, I, and J, which had a pH around 3.5. We did not find the direct connection between physical/chemical stability and water content and the connection with pH was rather speculative; however, it seemed that higher pH caused mixture instability.

4. Conclusions

In order to overcome the polymorphism issues of ivabradine hydrochloride, we concentrated on the preparation of a stable co-crystalline solid form. We identified and characterized two novel co-crystals of ivabradine hydrochloride, with (*S*)- and (*R*)-mandelic acid, IClSM and IClRM respectively. From a comparison of their properties, IClSM was selected for further studies. The co-crystal IClSM proved to be as stable as ivabradine hydrochloride form γ, which was identified in the original drug product. Therefore, the robust preparation of the co-crystal followed, as well as formulation with the excipients. We decided to attempt to prepare the co-crystal directly during the formulation process by granulation with ethanol. IClSM co-crystal proved to be able to form, even when its components were diluted by excess of excipients. To assess the possible negative effect of in situ co-crystal preparation on overall stability, we compared the stability of both pre-prepared and in situ prepared co-crystal formulations. Since we found that the influence was minimal and that the composition of excipients had much stronger influence on the tablet performance, the in situ co-crystal preparation showed as an effective and convenient means of robust preparation of a co-crystal of interest, during the wet granulation process in drug production. Moreover, such an approach is advantageous for generic product development, since all metastable polymorphs can be used for co-crystal preparation and undesired polymorphic impurities are avoided.

Supplementary Materials: The following are available online at www.mdpi.com/2073-4352/7/1/13/s1. Figure S1: The XRPD patterns of co-crystal IClSM (middle, blue); starting components, ivabradin hydrochloride form δd top, black); and (*S*)-mandelic acid (bottom, orange). Figure S2: The final Rietveld plot of the co-crystal IClSM, showing the measured and the calculated data. The calculated Bragg positions are shown by vertical bars. Figure S3: The DSC curve of the co-crystal IClSM. Figure S4: The DVS curve of the co-crystal IClSM. Figure S5: The Raman spectra of IClSM (blue curve), ivabradine hydrochloride δd (black dashed curve), and (*S*)-mandelic acid (orange dash dotted curve). Figure S6: The infrared (IR) spectra of IClSM (blue curve), ivabradine hydrochloride δd (black dashed curve), and (*S*)-mandelic acid (orange dotted curve). Figure S7: The XRPD patterns of co-crystal IClRM (middle, green); starting components, ivabradin hydrochloride form δd (top, black); and (*R*)-mandelic acid (bottom, orange). Figure S8: The final Rietveld plot of the co-crystal IClSM, showing the measured and the calculated data. Figure S9: The DSC curve of the co-crystal IClRM. Figure S10: The DVS curve of the co-crystal IClRM. Figure S11: The Raman spectra of IClRM (green curve), ivabradine hydrochloride δd (black dashed curve), and (*R*)-mandelic acid (orange dotted curve). Figure S12: The IR spectra of IClRM (green curve), ivabradine hydrochloride δd (black dashed curve), and (*R*)-mandelic acid (orange dotted curve). Figure S13: The XRPD patterns of IVA HCl δd (black), IClSM (blue) and IClRM (green). Figure S14: Comparison of Raman spectra of IClSM (blue) and IClRM (green). Figure S15: Comparison of IR spectra of IClSM (blue) and IClRM (green). Figure S16: In-house small-scale high-shear granulator. Figure S17: The XRPD patterns of pure IClSM (green) and granulation mixtures with lactose monohydrate. Figure S18: The detail of XRPD patterns of pure IClSM (green), IClSM + lactose monohydrate mixtures, and IVA HCl + (*S*)-mandelic acid + lactose monohydrate mixtures (red and magenta). Figure S19: The detail of XRPD patterns of pure IClSM (green), IClSM + lactose monohydrate mixtures after granulation (black, blue, turquoise, grey, teal), and IVA HCl + (*S*)-mandelic acid + lactose monohydrate mixtures (red, violet, and magenta). Table S1: Comparison of long-term (25 °C/60% RH) and accelerated (40 °C/75% RH) physical stability of IClSM co-crystal and polymorphic form δd. Table S2: Characterization (pH, water content, solid form (XRPD), chemical purity (UPLC)) of formulation mixtures A–C, containing IClSM co-crystal. Table S3: Characterization of formulation mixtures D–J.

Acknowledgments: We would like to acknowledge the Solid State department of Zentiva, our big thanks go to Tomáš Pekárek, Marcela Tkadlecová, Jaroslava Svobodová and Lukáš Krejčík. This work was also supported by the Grant Agency of Czech Republic, Grant No. 106/16/10035S and received financial support from specific university research (MSMT No. 20-SVV/2016).

Author Contributions: Veronika Sládková and Ondřej Dammer conceived and designed the experiments; Eliška Skořepová was responsible for the crystallographic parts; Gregor Sedmak proposed the formulation composition and Bohumil Kratochvíl contributed by project coordination; Veronika Sládková, Ondřej Dammer and Eliška Skořepová wrote the paper.

Conflicts of Interest: The authors declare no conflict of interest.

References

1. Wouters, J.; Quere, L. *Pharmaceutical Salts and Co-Crystals 2012*; Royal Society of Chemistry: Cambridge, UK, 2012; p. 391.
2. Friščic, T.; Jones, W. Recent Advances in Understanding the Mechanism of Cocrystal Formation via Grinding. *Cryst. Growth Des.* **2009**, *9*, 1621–1637. [CrossRef]
3. Etter, M.C.; Reutzel, S.M.; Choo, C.G. Self-organization of adenine and thymine in the solid state. *J. Am. Chem. Soc.* **1993**, *115*, 4411–4412. [CrossRef]
4. Trask, A.V.; Motherwell, W.D.S.; Jones, W. Solvent-drop grinding: Green polymorph control of cocrystallization. *Chem. Commun.* **2004**, 890–891. [CrossRef] [PubMed]
5. Berry, D.J.; Horton, P.N.; Hursthouse, M.B.; Storey, R.; Jones, W.; Friščić, T.; Seaton, C.C.; Clegg, W.; Harrington, R.W.; Coles, S.J. Applying Hot-Stage Microscopy to Co-Crystal Screening: A Study of Nicotinamide with Seven Active Pharmaceutical Ingredients. *Cryst. Growth Des.* **2008**, *8*, 1697–1712. [CrossRef]
6. Lu, E.; Rodriguez-Hornedo, N.; Suryanarayanan, R. A rapid thermal method for cocrystal screening. *CrystEngComm* **2008**, *10*, 665–668. [CrossRef]
7. Childs, S.L.; Rodriguez-Hornedo, N.; Reddy, L.S.; Jayasankar, A.; Maheshwari, C.; McCausland, L.; Shipplett, R.; Stahly, B.C. Screening strategies based on solubility and solution composition generate pharmaceutically acceptable cocrystals of carbamazepine. *CrystEngComm* **2008**, *10*, 856–864. [CrossRef]
8. Duggirala, N.K.; Perry, M.L.; Almarsson, O.; Zaworotko, M.J. Hydrogen Bond Hierarchy: Persistent Phenol··· Chloride Hydrogen Bonds in the Presence of Carboxylic Acid Moieties. *Cryst. Growth Des.* **2015**, *15*, 4341–4354. [CrossRef]
9. Braga, D.; Grepioni, F.; Maini, L.; Prosperi, S.; Gobetto, R.; Chierotti, M.R. From unexpected reactions to a new family of ionic co-crystals: The case of barbituric acid with alkali bromides and caesium iodide. *Chem. Commun. (Camb.)* **2010**, *46*, 7715–7717. [CrossRef] [PubMed]
10. Sladkova, V.; Skalicka, T.; Skorepova, E.; Cejka, J.; Eigner, V.; Kratochvil, B. Systematic solvate screening of trospium chloride: Discovering hydrates of a long-established pharmaceutical. *CrystEngComm* **2015**, *17*, 4712–4721. [CrossRef]
11. Tieger, E.; Kiss, V.; Pokol, G.; Finta, Z.; Dušek, M.; Rohlíček, J.; Skořepová, E.; Brázda, P. Studies on the crystal structure and arrangement of water in sitagliptin L-tartrate hydrates. *CrystEngComm* **2016**, *18*, 3819–3831. [CrossRef]
12. Childs, S.L. Crystal engineering approach to forming cocrystals of amine hydrochlorides with organic acids. Molecular complexes of fluoxetine hydrochloride with benzoic, succinic, and fumaric acids. *J. Am. Chem. Soc.* **2004**, *126*, 13335–13342. [CrossRef] [PubMed]
13. Sládková, V.; Cibulková, J.; Eigner, V.; Šturc, A.; Kratochvíl, B.; Rohlíček, J. Application and Comparison of Cocrystallization Techniques on Trospium Chloride Cocrystals. *Cryst. Growth Des.* **2014**, *14*, 2931–2936. [CrossRef]
14. Skorepova, E.; Husak, M.; Cejka, J.; Zamostny, P.; Kratochvil, B. Increasing dissolution of trospium chloride by co-crystallization with urea. *J. Cryst. Growth* **2014**, *399*, 19–26. [CrossRef]
15. Brittain, H.G. Pharmaceutical cocrystals: The coming wave of new drug substances. *J. Pharm. Sci.* **2013**, *102*, 311–317. [CrossRef] [PubMed]
16. Pop, M.; Sieger, P.; Cains, P.W. Tiotropium fumarate: An interesting pharmaceutical co-crystal. *J. Pharm. Sci.* **2009**, *98*, 1820–1834. [CrossRef] [PubMed]
17. Cruz-Cabeza, A.J.; Reutzel-Edens, S.M.; Bernstein, J. Facts and fictions about polymorphism. *Chem. Soc. Rev.* **2015**, *44*, 8619–8635. [CrossRef] [PubMed]
18. Prohens, R.; Barbas, R.; Portell, A.; Font-Bardia, M.; Alcobé, X.; Puigjaner, C. Polymorphism of Cocrystals: The Promiscuous Behavior of Agomelatine. *Cryst. Growth Des.* **2016**, *16*, 1063–1070. [CrossRef]
19. Peglion, J.L.; Vian, J.; Vilaine, J.P.; Villeneuve, N.; Janiak, P.; Bidouard, J.P. *Preparation of N-[(Benzocyclobutylalkyl) amino]alkyl]tetrahydro-3-benzazepin-2-ones and Analogs as Cardiovascular Agents*; Adir et Compagnie Patents: Courbevoie, France, 1993; p. 24.
20. Horvath, S.; Auguste, M.-N.; Damien, G. *Process for the Preparation of the Polymorphic γ-Crystalline Form of Ivabradine Hydrochloride and Pharmaceutical Compositions Containing It*; Les Laboratoires Servier: Suresnes, France, 2006; p. 4.

21. Lerestif, J.-M.; Lecouve, J.-P.; Souvie, J.-C.; Brigot, D.; Horvath, S.; Auguste, M.-N.; Damien, G. *Process for the Preparation of Ivabradine via Hydrogenation of Oxobenzazepinepropanal Acetal Derivative and Coupling with Dimethoxycyclobutabenzenemethanamine*; Les Laboratoires Servier: Suresnes, France, 2005; p. 6.
22. Horvath, S.; Auguste, M.-N.; Damien, G. *Preparation of β-Crystalline Form of Ivabradine Hydrochloride for Pharmaceuticals*; Les Laboratoires Servier: Suresnes, France, 2006; p. 9.
23. Horvath, S.; Auguste, M.-N.; Damien, G. *Preparation of β-d Crystalline Form of Ivabradine Hydrochloride for Pharmaceuticals*; Les Laboratoires Servier: Suresnes, France, 2006; p. 8.
24. Horvath, S.; Auguste, M.-N.; Damien, G. *Preparation of γ-d Crystalline Form of Ivabradine Hydrochloride for Pharmaceutical Compositions*; Les Laboratoires Servier: Suresnes, France, 2006; p. 9.
25. Horvath, S.; Auguste, M.-N.; Damien, G. *Delta Crystalline Form of Ivabradine Hydrochloride*; Les Laboratoires Servier: Suresnes, France, 2007; p. 4.
26. Barreca, G.; Gatti, M.M.; Ventimiglia, G. *New Polymorph of Ivabradine Hydrochloride and Method for Its Preparation*; Chemo Research, S.L.: Madrid, Spain, 2014; p. 25.
27. Dwivedi, S.D.; Prasad, A.; Patel, M.S.; Sharma, P.R. *Preparation of a Polymorphic Form of Ivabradine Hydrochloride*; Chemical Indexing Equivalent to 160:166199 (IN); Cadila Healthcare Limited: Ahmedabad, India, 2012; p. 29.
28. Dwivedi, S.D.; Kumar, R.; Patel, S.T.; Shah, A.P.C. *Process for Preparation of Ivabradine Hydrochloride*; Cadila Healthcare Limited: Ahmedabad, India, 2008; p. 33.
29. Dwivedi, S.D.; Prasad, A.; Sharma, M.H.; Sharma, P.R.; Parihar, J.A. *Polymorphic Forms of Ivabradine Hydrochloride*; Chemical Indexing Equivalent to 159:172881 (IN); Cadila Healthcare Limited: Ahmedabad, India, 2013; p. 35.
30. Kotar-Jordan, B.; Gojak, U.; Smrkolj, M. *Novel Forms of Ivabradine Hydrochloride*; Krka: Novo Mesto, Slovenia, 2011; p. 36.
31. Chen, Y.; Hong, C.; Liu, D.; Zhu, W. *Ivabradine Hydrochloride New Crystal Form C, and Its Preparation Method*; Jiangsu Yutian Bio-Pharmaceutical Technology Co., Ltd.: Lianyungang, China, 2013; p. 9.
32. Zhang, X.; Cui, D.; Zhang, T. *S Crystal Form of Ivabradine Hydrochloride, and Prepn. Method and Pharmaceutical Compn*; Beijing Lunarsun Pharmaceutical Co., Ltd.: Beijing, China, 2015; p. 23.
33. Prohens Lopez, R.; Puigjaner Vallet, C.; Barbas Canero, R.; Del Rio Pericacho, J.L.; Marti, J. *Preparation of Ivabradine Hydrochloride Form IV*; Urquima S.A.: Barcelona, Spain, 2013; p. 30.
34. Wieser, J.; Griesser, U.; Enders, M.; Kahlenberg, V. *Preparation of Acetone Solvate of Ivabradine Hydrochloride*; Sandoz AG: Rotkreuz ZG, Switzerland, 2013; p. 44.
35. Sun, P.; Chen, Y.; Yu, G. *Ivabradine Sulfate, Its Type I Crystal and Preparation Method Thereof*; Jiangsu Hengrui Medicine Co., Ltd.: Lianyungang, China, 2010; p. 8.
36. Singh, S.P.; Singh, G.; Wadhwa, L. *Process for the Preparation of Ivabradine Hydrochloride and Related Polymorphs*; IND-Swift Laboratories Limited: Chandigarh, India, 2008; p. 22.
37. Singh, G.; Singh, S.P.; Wadhwa, L. *Acid Addition Salts of Ivabradine and Preparation Thereof*; IND-Swift Laboratories Limited: Chandigarh, India, 2011; p. 24.
38. Gidwani, R.M.; Kolhatkar, M.V.; Meergans, D.; Stefan, R.; Geier, J. *Ivabradine-Containing Pharmaceutical Composition with Modified Release*; Ratiopharm GmbH: Ulm, Germany, 2011; p. 28.
39. Smrkolj, M.; Gojak, U.; Kotar-Jordan, B. *Pharmaceutical Compositions Comprising Ivabradine Hydrobromide*; Krka: Tovarna Zdravil, d.d., Slovenia, 2009; p. 34.
40. Alhalaweh, A.; Velaga, S.P. Formation of Cocrystals from Stoichiometric Solutions of Incongruently Saturating Systems by Spray Drying. *Cryst. Growth Des.* **2010**, *10*, 3302–3305. [CrossRef]
41. Daurio, D.; Medina, C.; Saw, R.; Nagapudi, K.; Alvarez-Núñez, F. Application of Twin Screw Extrusion in the Manufacture of Cocrystals, Part I: Four Case Studies. *Pharmaceutics* **2011**, *3*, 582–600. [CrossRef] [PubMed]
42. Allen, F.H.; Motherwell, W.D.S. Applications of the Cambridge Structural Database in organic chemistry and crystal chemistry. *Acta Crystallogr. Sect. B* **2002**, *58*, 407–422. [CrossRef]
43. Duval, D.; Hennig, P.; Bouchet, J.P.; Vian, J.; Peglion, J.L.; Volland, J.P.; Platzer, N.; Guilhem, J. Stereochemical Study of a Bradicardisant Benzazepine-Type Drug. X-ray Structure of the Chloride Salt and High-Field NMR Study of the Stereochemistry in Solution. *Magn. Reson. Chem.* **1997**, *35*, 175–183. [CrossRef]
44. Hu, X.; Gu, J.; Jin, Z.; Huang, Y.; Huang, J. *Stable Crystal Form II of Ivabradine Hydrochloride and Preparation Method Thereof*; Zhejiang Jingxin Pharmaceutical Co., Ltd.: Shaoxing, China, 2013; p. 40.

45. Masciocchi, N.; Aulisio, A.; Bertolini, G.; Sada, M.; Garis, F.; Malpezzi, L. Disclosing the extensive crystal chemistry of Ivabradine hydrochloride, in its pure and solvated phases. *Powder Diffr.* **2013**, *28*, 200–206. [CrossRef]
46. Council of Europe. *European Pharmacopoeia*, 7th ed.; Council of Europe: Strasbourg, France, 2012.
47. Skorepova, E.; Husak, M.; Ridvan, L.; Tkadlecova, M.; Havlicek, J.; Dusek, M. Iodine salts of a pharmaceutical compound agomelatine: Effect of symmetric H-bond on amide protonation. *CrystEngComm* **2016**, *18*, 4518–4529. [CrossRef]
48. Lubach, J.W.; Xu, D.; Segmuller, B.E.; Munson, E.J. Investigation of the effects of pharmaceutical processing upon solid-state NMR relaxation times and implications to solid-state formulation stability. *J. Pharm. Sci.* **2007**, *96*, 777–787. [CrossRef] [PubMed]